Int J Cardiovasc Imaging (2012) 28:1307–1314
DOI 10.1007/s10554-011-9981-4

ORIGINAL PAPER

Analysis of 1 year virtual histology changes in coronary plaque located behind the struts of the everolimus eluting bioresorbable vascular scaffold

Salvatore Brugaletta · Josep Gomez-Lara · Hector M. Garcia-Garcia · Jung Ho Heo · Vasim Farooq · Robert J. van Geuns · Bernard Chevalier · Stephan Windecker · Dougal McClean · Leif Thuesen · Robert Whitbourn · Ian Meredith · Cecile Dorange · Susan Veldhof · Richard Rapoza · John A. Ormiston · Patrick W. Serruys

Received: 4 July 2011 / Accepted: 14 November 2011 / Published online: 23 November 2011

Abstract Serial intravascular ultrasound virtual histology (IVUS-VH) after implantation of metallic stents has been unable to show any changes in the composition of the scaffolded plaque overtime. The everolimus-eluting ABSORB scaffold potentially allows for the formation of new fibrotic tissue on the scaffolded coronary plaque during bioresorption. We examined the 12 month IVUS-VH changes in composition of the plaque behind the struts (PBS) following the implantation of the ABSORB scaffold. Using IVUS-VH and dedicated software, the composition of the PBS was analyzed in all patients from the ABSORB Cohort B2 trial, who were imaged with a commercially available IVUS-VH console (s5i system, Volcano Corporation, Rancho Cordova, CA, USA), immediately post-ABSORB implantation and at 12 month follow-up. Paired IVUS-VH data, recorded with s5i system, were available in 17 patients (18 lesions). The analysis demonstrated an increase in mean PBS area (2.39 ± 1.85 mm^2 vs. 2.76 ± 1.79 mm^2, $P = 0.078$) and a

S. Brugaletta · J. Gomez-Lara · H. M. Garcia-Garcia · J. H. Heo · V. Farooq · R. J. van Geuns · P. W. Serruys (✉)
Department of Interventional Cardiology, Thoraxcenter, Erasmus MC, 's Gravendijkwal 230, 3015 Rotterdam, CE, The Netherlands
e-mail: p.w.j.c.serruys@erasmusmc.nl

S. Brugaletta
Department of Cardiology, Thorax Institute Hospital Clinic, Barcelona, Spain

H. M. Garcia-Garcia
Cardialysis B.V., Rotterdam, The Netherlands

B. Chevalier
Institut Cardiovasculaire Paris Sud, Massy, France

S. Windecker
Bern University Hospital, Bern, Switzerland

D. McClean
Chrischurch Hospital, Christchurch, New Zealand

L. Thuesen
Skejby Sygehus, Aarhus University Hospital, Aarhus, Denmark

R. Whitbourn
St Vincents Hospital, Fitzroy, Australia

I. Meredith
Monash Cardiovascular Research Centre, Melbourne, Australia

C. Dorange · S. Veldhof
Abbott Vascular, Diegem, Belgium

R. Rapoza
Abbott Vascular, Santa Clara, CA, USA

J. A. Ormiston
Department of Cardiology, Auckland City Hospital, Auckland, New Zealand

reduction in the mean lumen area (6.37 ± 0.90 mm^2 vs. 5.98 ± 0.97 mm^2, $P = 0.006$). Conversely, a significant decrease of 16 and 30% in necrotic core (NC) and dense calcium (DC) content, respectively, were evident (median % NC from 43.24 to 36.06%, $P = 0.016$; median % DC from 20.28 to 11.36%, $P = 0.002$). Serial IVUS-VH analyses of plaque located behind the ABSORB struts at 12-month demonstrated an increase in plaque area with a decrease in its NC and DC content. Larger studies are required to investigate the clinical impact of these findings.

Keywords Bioresorbable vascular scaffold · Coronary plaque · IVUS-VH · Everolimus · Necrotic core

Introduction

Percutaneous treatment of atherosclerotic lesions with use of metallic stents leads to a stretching of coronary plaques by baro-trauma [1]. The implantation of a foreign body, such as a metallic stent, is also known to induce an inflammatory response adjacent to the struts [2–4]. However, serial analyses by intravascular ultrasound virtual histology (IVUS-VH) have demonstrated no changes at 10 months in the VH components of coronary plaques after bare metal or drug eluting stent implantation [5, 6].

The new everolimus-eluting bioresorbable vascular scaffold (ABSORB, Abbott Vascular, Santa Clara, CA) has been developed with the intention to provide temporary lumen scaffolding and, in contrast to metallic platform stents, to allow late lumen enlargement and restoration of normal vasomotion post bioresorption [7]. In the ABSORB Cohort A trial a non significant reduction in the VH-derived necrotic core (NC) was demonstrated between 6 month and 2 year follow-up [7, 8]. However, as the polymeric struts are mistakenly recognized by IVUS-VH as dense calcium and necrotic core and are progressively bioresorbed, a concomitant result of scaffold bioresorption and plaque modification has to be taken into account for the correct interpretation of VH changes over time [9, 10].

Conversely, in the ABSORB Cohort B trial, a customized software, allowing for the exclusion of the dense calcium and necrotic core due to the temporary presence of the scaffold from the quantification of the VH-plaque behind the polymeric struts, was used. At 6-month follow-up a slight increase in the plaque area, in particular in its relative NC content, was evident [11]. The 12 month follow-up of this trial recently demonstrated a further increase in the plaque size but with clear signs of pharmacologically induced vasomotion of the scaffolded segment, suggesting loss of the mechanical integrity and radial forces of the scaffold and favourable changes in the composition of the plaque [12].

The aim of this study was therefore to analyze the 12 month changes in the VH composition of only the plaque behind the polymeric struts.

Methods

Study population

The ABSORB Cohort B trial enrolled patients older than 18 years, with a diagnosis of stable, unstable or silent ischemia, subdivided in two subgroups: the first group (Cohort B1) underwent invasive imaging such as quantitative coronary angiography, IVUS, IVUS-VH and optical coherence tomography at 6 months whereas the second group (Cohort B2) underwent the same invasive imaging at 12 months. For the present analysis, we screened patients from ABSORB Cohort B2 with paired post-implantation and 12 month follow-up IVUS-VH.

Briefly, all lesions were de novo, in a native coronary artery with a reference vessel diameter of 3.0 mm, with a percentage diameter stenosis $\geq$50 and $<$100% and a thrombolysis in myocardial infarction flow grade of $\geq$1. All lesions were treated by implantation of the ABSORB scaffold 1.1 (3.0 × 18 mm) [7, 13]. Major exclusion criteria were: patients presenting with an acute myocardial infarction, unstable arrhythmias or patients who had left ventricular ejection fraction $\leq$30%, restenotic lesions, lesions located in the left main coronary artery, lesions involving a side branch $>$2 mm in diameter, and the presence of thrombus or another clinically significant stenosis in the target vessel. The trial was approved by the ethics committee at each participating institution and each patient gave written informed consent before inclusion.

Imaging acquisition and analysis

IVUS-VH post-implantation and at 12 month follow-up were acquired with a phased array 20 MHz intravascular ultrasound catheter (EagleEye™; Volcano Corporation, Rancho Cordova, CA, USA) using an automated pullback of 0.5 mm per second. The baseline and one-year follow-up region of interest were matched by use of anatomical landmarks. The radiofrequency data, required for VH analysis, were acquired during the IVUS pullback and raw radiofrequency data capture gated to the R wave (In-Vision Gold, Volcano). These files were stored on DVD and sent to an independent core laboratory for analyses (Cardialysis, BV, Rotterdam, The Netherlands).

The data were analyzed by the QIVUs software (Medis, Leiden, The Netherlands). This allowed the user to draw, in a semi-automatic fashion, a third contour (i.e. the scaffold contour). One limitation of this software, however, is its ability to read only IVUS-VH data acquired using a specific commercially available IVUS-VH console (s5i system, Volcano Corporation, Rancho Cordova, CA, USA).

Three different contours were drawn (lumen, scaffold and external elastic membrane) by experienced IVUS analysts blinded to the time of acquisition (e.g. baseline or 12 month follow-up) [14]. Reproducibility of these measurements using this software has been previously demonstrated to be good [11]. Four tissue components (necrotic core NC—red; dense calcium DC—white; fibrous FT—green; and fibrofatty FF—light green) were identified with autoregressive classification system. Each individual tissue component was quantified and colour coded in all IVUS cross sections [7, 15]. As previously described, the scaffold contour was drawn behind the polymeric struts of the ABSORB scaffold, excluding the polymeric struts and their ultrasonic signature from the quantification of the VH components of the plaque behind the struts (PBS). The PBS was calculated as the sum of all IVUS-VH components, excluding the grey media stripe seen with IVUS-VH.

In addition, we qualitatively evaluated the presence of necrotic core in contact with the lumen, defined as a confluent necrotic core >10% of plaque area without evidence of overlying non-necrotic core tissue in the treated segment and in the edges (5 mm length adjacent to each ABSORB scaffold edge), as previously reported [6, 11]. Importantly, as the polymeric struts are recognized as dense calcium surrounded by necrotic core, this surrounding necrotic core, with the help of the corresponding grey-scale image, was not interpreted as necrotic core in contact with the lumen [5, 6, 9, 11].

Statistical analysis

Discrete variables are presented as counts and percentages. Continuous variables are presented as means ± standard deviation (SD) or median and interquartile range, according to their normal or not normal distribution. Normal distribution of continuous variables was tested by the Kolgomorov-Smirnov test. The ratio between the number of frames with necrotic core in contact with the lumen and the total number of frames analyzed has been defined as the incidence of necrotic core in contact with the lumen for the treated segment and the edges. Paired comparisons between post-procedure and 12-month follow-up were done by paired t-test or Wilcoxon signed rank test, where appropriate. Correlation between parameters was performed by the Spearman test. A two-side P value of less than 0.05 indicated statistical significance. Statistical analyses were performed with the use of SPSS 16.0 software (SPSS Inc., Chicago IL, USA).

Results

Baseline clinical and angiographic characteristics

Overall, forty-six patients had paired post-ABSORB implantation and 12 month follow-up IVUS-VH data. Of these patients, only 17 patients (18 lesions) were imaged using the s5i system and therefore were included in the present study. Table 1 shows their clinical and angiographic data. No differences were found in the clinical and angiographic data between patients included and excluded from the analysis.

Grey-scale IVUS and IVUS-VH analyses (Table 2)

PBS tended to increase from baseline to 12 months follow-up (from 2.39 ± 1.85 to 2.76 ± 1.79 mm^2; $P = 0.078$) with a significant reduction in lumen area (from 6.37 ± 0.90 to 5.98 ± 0.97 mm^2; $P = 0.006$).

Table 1 Baseline clinical and angiographic characteristics

	Patients (n = 17) Lesions (n = 18)
Age (years)	
Mean ± SD (n)	60.5 ± 9.1
Men, n (%)	14 (82)
Smokers, n (%)	1 (6)
Diabetes, n (%)	2 (12)
Hypertension requiring medication, n (%)	11 (65)
Hyperlipidaemia requiring medication, n (%)	11 (65)
Previous PCI, n (%)	2 (11)
Previous myocardial infarction, n (%)	2 (13)
Stable angina, n (%)	11 (65)
Unstable angina, n (%)	4 (24)
Silent ischaemia, n (%)	2 (12)
Target vessel, n (%)	
Left anterior descending	11 (61)
Left circumflex	2 (11)
Right coronary artery	5 (28)
AHA/ACC lesion classification, n (%)	
A	0 (0)
B1	11 (65)
B2	5 (29)
Medical treatment, n (%)	
ß-blockers	13 (80)
ACE-inhibitors	9 (55)
Statins	16 (94)

SD standard deviation, *PCI* percutaneous coronary intervention, *AHA/ACC* American Heart Association/American College of Cardiology

No changes were found in the EEM area (from 14.08 ± 3.14 to 14.32 ± 3.13 mm^2; $P = 0.349$).

In the IVUS-VH analysis of the PBS, there was a significant increase in the absolute and relative content of fibrous and fibrofatty tissue. Conversely, there was a significant decrease in the relative content of necrotic core and dense calcium (Fig. 1).

Whilst there was no relationship between the changes in NC and DC areas and in the PBS area between baseline and follow-up (Spearman rho = 0.24, $P = 0.336$ for NC; Spearman rho = 0.15, $P = 0.553$ for DC), there was a significant relationship between the changes in FT and FF area and in the PBS area (Spearman rho = 0.87, $P < 0.001$ for FT; Spearman rho = 0.78, $P < 0.001$ for FF).

Incidence of necrotic core in contact with the lumen

Overall there was a reduction in necrotic core in contact with the lumen not only at the scaffold site, but also at the proximal and distal reference segments (Fig. 2). In particular the reduction of NC in contact with the lumen approached a statistical significance in the proximal reference segment ($P = 0.09$) (Fig. 3).

Intra-observer and inter-observer variabilities yielded good concordance for necrotic core in contact with the lumen ($\kappa = 0.86$ and $\kappa = 0.80$, respectively).

Discussion

The major finding of our study is that at 12 month follow-up there is an increase of plaque located behind the polymeric struts of the ABSORB scaffold, mainly due to an increase in its fibrous and fibrofatty content. Conversely, there is a significant decrease in necrotic core and dense calcium tissue.

The use of IVUS-VH in the study of the coronary plaque after stent/scaffold implantation is challenging, as metallic and polymeric struts are detected as dense calcium, surrounded by necrotic core and are accounted for the quantification of the plaque VH component [6, 9]. In addition, with bioresorbable polymeric struts, the weight of the scaffold in the quantification of the VH plaque components changes at various time points according to the scaffold bioresorption. Consequently, a reduction in the dense calcium and necrotic core content of the plaque may be an artifactual result of this process [7–9]. The semi-automatic introduction of a third contour, excluding the scaffold from the analysis of the VH plaque, allows us to overcome these problems.

Using this methodology, at 6 month follow-up we demonstrated an increase in plaque area and in all the VH components, without an increase of the necrotic core in contact with the lumen [11]. At 12 months, we conversely found a significant decrease in necrotic core and dense calcium, despite an increase in plaque area. The reduction of necrotic core was also accompanied by a reduction in the necrotic core in contact with the lumen either in the scaffold region or within

Table 2 IVUS analysis in the scaffold segment at baseline and follow-up (n = 18 lesions)

	Baseline	Follow-up	Difference % based on individual data	*P* value
Mean EEM area (mm^2)	14.08 ± 3.14	14.32 ± 3.13	2.54 ± 12.77	0.349
PBS area (mm^2)	2.39 ± 1.85	2.76 ± 1.79	7.31 (−3.86 to 26.54)	0.078
Mean Lumen area (mm^2)	6.37 ± 0.90	5.98 ± 0.97	−6.19 ± 7.13	0.006
Fibrous tissue (mm^2)	0.59 (0.28–1.11)	1.01 (0.59–1.94)	42.76 (14.91–122.31)	0.004
Fibrous tissue (%)	28.10 (26.15–33.31)	43.90 (34.82–51.35)	45.02 (13.06–62.50)	0.001
Fibro-fatty tissue (mm^2)	0.04 (0.01–0.14)	0.12 (0.06–0.22)	200.14 (50.52–819.11)	0.011
Fibro-fatty tissue (%)	1.82 (0.83–4.08)	5.16 (3.85–6.86)	163.77 (56.34–513.07)	0.004
Necrotic core (mm^2)	0.89 (0.52–1.53)	0.81 (0.59–1.41)	−8.29 (−18.64–11.35)	0.369
Necrotic core (%)	43.24 (38.77–52.71)	36.06 (32.53–43.79)	−15.59 (−27.87–1.06)	0.016
Dense calcium (mm^2)	0.39 (0.08–0.55)	0.27 (0.15–0.46)	−20.94 (−42.72–14.30)	0.048
Dense calcium (%)	20.28 (11.95–27.04)	11.36 (8.59–18.78)	−30.16 (−50.71–−20.20)	0.002

Data are expressed as mean ± SD or median and interquartile range, according to their normal or not normal distribution, respectively

EEM external elastic membrane, *PBS* plaque behind struts

the proximal/distal reference segments. Of note is that dense calcium is a frequent finding within the necrotic core region; in this case it is frequently "speckled" which can be due to calcification of a "nidus" of macrophages, a sign associated with plaque instability and rupture [16]. The reduction of dense calcium found in our analysis was probably mainly due to the reduction of this type of dense calcium within the necrotic core area (Fig. 1). However, as calcium tends to be stable over short follow-up, another possible explanation could be that scaffold bioresorption influences the radiofrequency backscattering signal behind the scaffold, producing a reduction in dense calcium. At 12-month follow-up there was also an increase in fibrotic tissue content of the plaque. Previous optical coherence tomography studies have shown that polymeric struts apposed and embedded in the vessel wall become covered by neointima hyperplasia that also intersperses between the polymeric struts [17, 18].

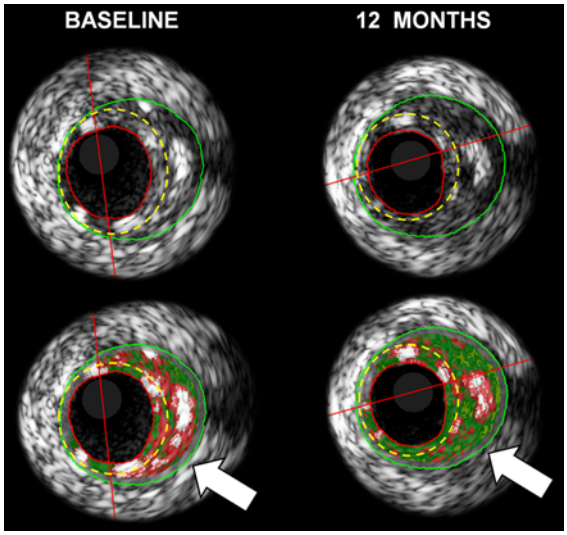

Fig. 1 Example of reduction of necrotic core and dense calcium in the plaque behind the polymeric struts (*white arrows*). Note also the increase of plaque size with predominant content of fibrous tissue. Yellow contour is drawn behind the ABSORB polymeric struts in a semi-automatic way by the dedicated software, excluding struts from the VH quantification of the plaque behind

Everolimus is probably the major component in the reduction of VH-derived necrotic core. Verheye et al.

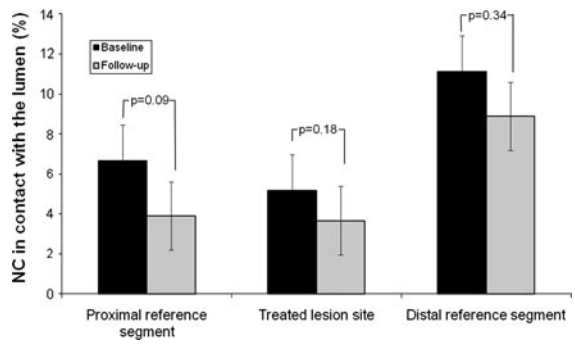

Fig. 2 Incidence of segments with necrotic core in contact with the lumen at baseline and follow-up

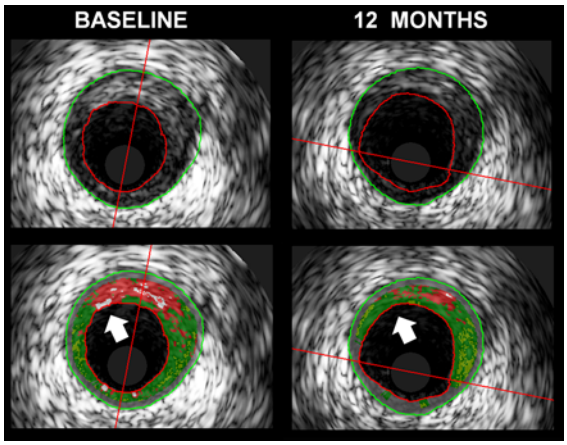

Fig. 3 Representative IVUS-VH image of necrotic core in contact with the lumen in the proximal reference segment at baseline and which has disappeared at follow-up

showed in rabbit atherosclerotic plaques that a stent-based delivery of everolimus leads to a marked reduction in macrophage content without altering the amount of smooth muscle cells, namely inducing autophagy by mTOR inhibition. [19, 20] This autophagy of macrophages is classically described as a process of vacuolization of the cytoplasm with formation of auto-phagosome, digesting the surrounding atherosclerotic debris. This observation is important in the context of plaque stabilization, as it is generally assumed that the presence of macrophages triggers plaque destabilization [21]. In addition, the 12 month inflammatory reaction after ABSORB implantation in a porcine model has been shown to be lower than for metallic stents, in which the inflammatory process is prolonged [22]. These pathological findings from animal studies are in line with the present reduction in the necrotic core content of the atherosclerotic plaque at 12 month follow-up after ABSORB implantation, where the favourable effects of everolimus are combined with a bioresorbable platform [2–4]. It is noteworthy that the lack of everolimus effect on the smooth muscle cells may be the basis of the preserved pharmacologically induced vasomotion of the scaffold segment, as highlighted at the 12-month follow-up [12].

Statin treatment, that was used in most of the patients, should be considered as another possible explanation of our findings, in particular of the reduction in necrotic core, as previously shown [23]. Statin therapy could also explain the reduction in the necrotic core in contact with the lumen in the segment proximal to the device, as elution of everolimus is more frequent distal than proximal to the device [1].

Limitations

The present study included a small number of patients. IVUS-VH data pre-ABSORB implantation were not available. The interpretation of the backscattering signal from the plaque behind the polymeric struts by the IVUS-VH software may be influenced by the presence of the scaffold. IVUS-VH has not been validated to assess plaque composition behind scaffold struts and to identify bioresorbable struts. In addition struts bioresorption may account for the changes in the radiofrequency backscattering signal in the plaque behind.

Conclusions

At 12 months after ABSORB implantation, there was a slight increase in plaque area located behind the polymeric struts. Nevertheless, the necrotic core and dense calcium content of the plaque decreased significantly. These findings are compatible with the everolimus-induced autophagy of macrophages and subsequent reduction of inflammatory microenvironment of atherosclerotic plaque. The ability to decrease necrotic core content of coronary plaque without the permanent presence of metal may have important clinical implications in atherosclerosis treatment. Validation of the actual findings is needed and further studies with larger sample sizes and longer clinical follow-up are required before the impact of these observations can be fully understood.

Acknowledgments The ABSORB Trial is sponsored and funded by Abbott Vascular, Santa Clara, California, USA.

Conflicts of interest Cecile Dorange, Susan Veldhof and Richard Rapoza are employees of Abbott Vascular. There are no conflicts of interest regarding specific financial interests that there are relevant to the work conducted or reported in this manuscript.

References

1. Moses JW, Leon MB, Popma JJ, Fitzgerald PJ, Holmes DR, O'Shaughnessy C, Caputo RP, Kereiakes DJ, Williams DO, Teirstein PS, Jaeger JL, Kuntz RE (2003) Sirolimus-eluting stents versus standard stents in patients with stenosis in a native coronary artery. N Engl J Med 349(14):1315–1323. doi:10.1056/NEJMoa035071
2. Finn AV, Nakazawa G, Joner M, Kolodgie FD, Mont EK, Gold HK, Virmani R (2007) Vascular responses to drug eluting stents: importance of delayed healing. Arterioscler Thromb Vasc Biol 27(7):1500–1510. doi:10.1161/ATVBAHA.107.144220
3. Joner M, Finn AV, Farb A, Mont EK, Kolodgie FD, Ladich E, Kutys R, Skorija K, Gold HK, Virmani R (2006) Pathology of drug-eluting stents in humans: delayed healing and late thrombotic risk. J Am Coll Cardiol 48(1):193–202. doi:10.1016/j.jacc.2006.03.042
4. Wilson GJ, Nakazawa G, Schwartz RS, Huibregtse B, Poff B, Herbst TJ, Baim DS, Virmani R (2009) Comparison of inflammatory response after implantation of sirolimus- and paclitaxel-eluting stents in porcine coronary arteries. Circulation 120(2):141–149. doi:10.1161/CIRCULATIONAHA.107.730010 (141–142)
5. Kubo T, Maehara A, Mintz GS, Garcia-Garcia HM, Serruys PW, Suzuki T, Klauss V, Sumitsuji S, Lerman A, Marso SP, Margolis MP, Margolis JR, Foster MC, De Bruyne B, Leon MB, Stone GW (2010) Analysis of the long-term effects of drug-eluting stents on coronary arterial wall morphology as assessed by virtual histology intravascular ultrasound. Am Heart J 159(2):271–277. doi:10.1016/j.ahj.2009.11.008
6. Kim SW, Mintz GS, Hong YJ, Pakala R, Park KS, Pichard AD, Satler LF, Kent KM, Suddath WO, Waksman R, Weissman NJ (2008) The virtual histology intravascular ultrasound appearance of newly placed drug-eluting stents. Am J Cardiol 102(9):1182–1186. doi:10.1016/j.amjcard.2008.03.054
7. Serruys PW, Ormiston JA, Onuma Y, Regar E, Gonzalo N, Garcia-Garcia HM, Nieman K, Bruining N, Dorange C, Miquel-Hebert K, Veldhof S, Webster M, Thuesen L, Dudek D (2009) A bioabsorbable everolimus-eluting coronary stent system (ABSORB): 2-year outcomes and results from multiple imaging methods. Lancet 373(9667):897–910. doi:10.1016/S0140-6736(09)60325-1
8. Sarno G, Onuma Y, Garcia-Garcia HM, Garg S, Regar E, Thuesen L, Dudek D, Veldhof S, Dorange C, Ormiston JA, Serruys PW (2010) IVUS radiofrequency analysis in the evaluation of the polymeric struts of the bioabsorbable everolimus-eluting device during the bioabsorption process. Catheter Cardiovasc Interv 75(6):914–918. doi:10.1002/ccd.22332
9. Garcia-Garcia HM, Gonzalo N, Pawar R, Kukreja N, Dudek D, Thuesen L, Ormiston JA, Regar E, Serruys PW (2009) Assessment of the absorption process following bioabsorbable everolimus-eluting stent implantation: temporal changes in strain values and tissue composition using intravascular ultrasound radiofrequency data analysis. A substudy of the ABSORB clinical trial. EuroIntervention 4(4):443–448
10. Brugaletta S, Garcia-Garcia HM, Diletti R, Gomez-Lara J, Garg S, Onuma Y, Shin ES, Van Geuns RJ, De Bruyne B, Dudek D, Thuesen L, Chevalier B, McClean D, Windecker S, Whitbourn R, Dorange C, Veldhof S, Rapoza R, Sudhir K, Bruining N, Ormiston J, Serruys P (2011) Comparison between the first and second generation bioresorbable vascular scaffolds: a six month virtual histology study. EuroIntervention 6(9):1110–1116
11. Brugaletta S, Garcia-Garcia HM, Garg S, Gomez-Lara J, Diletti R, Onuma Y, van Geuns RJ, McClean D, Dudek D, Thuesen L, Chevalier B, Windecker S, Whitbourn R, Dorange C, Miquel-Hebert K, Sudhir K, Ormiston JA, Serruys PW (2011) Temporal changes of coronary artery plaque located behind the struts of the everolimus eluting bioresorbable vascular scaffold. Int J Cardiovasc Imaging 27(6):859–866. doi:10.1007/s10554-010-9724-y
12. Serruys PW, Onuma Y, Dudek D, Smits PC, Koolen J, Chevalier B, De Bruyne B, Thuesen L, McClean D, van Geuns RJ, Windecker S, Whitbourn R, Meredith C, Dorange C, Veldhof S, Miquel-Hebert K, Sudhir K, Garcia-Garcia HM, Ormiston JA (2011) Evaluation of the second generation of a bioresorbable everolimus-eluting vascular scaffold for the treatment of de novo coronary artery stenosis: 12-month clinical and imaging outcomes. J Am Coll Cardiol 58(15):1578–1588
13. Ormiston JA, Serruys PW, Regar E, Dudek D, Thuesen L, Webster MW, Onuma Y, Garcia-Garcia HM, McGreevy R, Veldhof S (2008) A bioabsorbable everolimus-eluting coronary stent system for patients with single de novo coronary artery lesions (ABSORB): a prospective open-label trial. Lancet 371(9616):899–907. doi:10.1016/S0140-6736(08)60415-8
14. Hausmann D, Lundkvist AJ, Friedrich GJ, Mullen WL, Fitzgerald PJ, Yock PG (1994) Intracoronary ultrasound imaging: intraobserver and interobserver variability of morphometric measurements. Am Heart J 128(4):674–680
15. Nair A, Kuban BD, Tuzcu EM, Schoenhagen P, Nissen SE, Vince DG (2002) Coronary plaque classification with intravascular ultrasound radiofrequency data analysis. Circulation 106(17):2200–2206
16. Garcia-Garcia HM, Mintz GS, Lerman A, Vince DG, Margolis MP, van Es GA, Morel MA, Nair A, Virmani R, Burke AP, Stone GW, Serruys PW (2009) Tissue characterisation using intravascular radiofrequency data analysis: recommendations for acquisition, analysis, interpretation and reporting. EuroIntervention 5(2):177–189
17. Gomez-Lara J, Brugaletta S, Diletti R, Garg S, Onuma Y, Gogas BD, van Geuns RJ, Dorange C, Veldhof S, Rapoza R, Whitbourn R, Windecker S, Garcia-Garcia HM, Regar E, Serruys PW (2011) A comparative assessment by optical coherence tomography of the performance of the first and second generation of the everolimus-eluting bioresorbable vascular scaffolds. Eur Heart J 32(3):294–304. doi:10.1093/eurheartj/ehq458
18. Serruys PW, Onuma Y, Ormiston JA, de Bruyne B, Regar E, Dudek D, Thuesen L, Smits PC, Chevalier B, McClean D, Koolen J, Windecker S, Whitbourn R, Meredith I, Dorange C, Veldhof S, Miquel-Hebert K, Rapoza R, Garcia-Garcia HM (2010) Evaluation of the second generation of a bioresorbable everolimus drug-eluting vascular scaffold for treatment of de novo coronary artery stenosis: six-month clinical and imaging outcomes. Circulation 122(22):2301–2312. doi:10.1161/CIRCULATIONAHA.110.970772

19. Verheye S, Martinet W, Kockx MM, Knaapen MW, Salu K, Timmermans JP, Ellis JT, Kilpatrick DL, De Meyer GR (2007) Selective clearance of macrophages in atherosclerotic plaques by autophagy. J Am Coll Cardiol 49(6): 706–715. doi:10.1016/j.jacc.2006.09.047
20. Martinet W, Verheye S, De Meyer GR (2007) Everolimus-induced mTOR inhibition selectively depletes macrophages in atherosclerotic plaques by autophagy. Autophagy 3(3): 241–244
21. Boyle JJ (2005) Macrophage activation in atherosclerosis: pathogenesis and pharmacology of plaque rupture. Curr Vasc Pharmacol 3(1):63–68
22. Onuma Y, Serruys PW, Perkins LE, Okamura T, Gonzalo N, Garcia-Garcia HM, Regar E, Kamberi M, Powers JC, Rapoza R, van Beusekom H, van der Giessen W, Virmani R (2010) Intracoronary optical coherence tomography and histology at 1 month and 2, 3, and 4 years after implantation of everolimus-eluting bioresorbable vascular scaffolds in a porcine coronary artery model: an attempt to decipher the human optical coherence tomography images in the ABSORB trial. Circulation 122(22):2288–2300. doi: 10.1161/CIRCULATIONAHA.109.921528
23. Hong MK, Park DW, Lee CW, Lee SW, Kim YH, Kang DH, Song JK, Kim JJ, Park SW, Park SJ (2009) Effects of statin treatments on coronary plaques assessed by volumetric virtual histology intravascular ultrasound analysis. JACC Cardiovasc Interv 2(7):679–688. doi:10.1016/j.jcin.2009.03.015